

# Geophysical Research Letters

## RESEARCH LETTER

10.1029/2019GL085725

### Key Points:

- European carbon sink estimated to be  $0.303 \pm 0.083$  GtC/yr
- Consistent assimilation of three observational data products into a terrestrial biosphere model
- SMOS soil moisture and vegetation optical depth reduce flux uncertainty by an additional 15–25% compared to assimilating CO<sub>2</sub> only

### Supporting Information:

- Supporting Information S1

### Correspondence to:

M. Scholze,

marko.scholze@nateko.lu.se

### Citation:

Scholze, M., Kaminski, T., Knorr, W., Voßbeck, M., Wu, M., Ferrazzoli, P., et al. (2019). Mean European carbon sink over 2010–2015 estimated by simultaneous assimilation of atmospheric CO<sub>2</sub>, soil moisture, and vegetation optical depth. *Geophysical Research Letters*, 46, 13,796–13,803. <https://doi.org/10.1029/2019GL085725>

Received 9 OCT 2019

Accepted 5 NOV 2019

Accepted article online 3 DEC 2019

Published online 4 DEC 2019

## Mean European Carbon Sink Over 2010–2015 Estimated by Simultaneous Assimilation of Atmospheric CO<sub>2</sub>, Soil Moisture, and Vegetation Optical Depth

**M. Scholze<sup>1</sup> , T. Kaminski<sup>2</sup>, W. Knorr<sup>1</sup> , M. Voßbeck<sup>2</sup> , M. Wu<sup>1</sup>, P. Ferrazzoli<sup>3</sup>, Y. Kerr<sup>4</sup>, A. Mialon<sup>4</sup>, P. Richaume<sup>4</sup>, N. Rodríguez-Fernández<sup>4</sup>, C. Vittucci<sup>3</sup>, J.-P. Wigneron<sup>5</sup>, S. Mecklenburg<sup>6</sup>, and M. Drusch<sup>7</sup>**

<sup>1</sup>Department of Physical Geography and Ecosystem Science, Lund University, Lund, Sweden, <sup>2</sup>The Inversion Lab, Hamburg, Germany, <sup>3</sup>Università di Roma Tor Vergata, Rome, Italy, <sup>4</sup>Centre d'Etudes Spatiales de la Biosphère (CESBIO), Université de Toulouse, Centre National d'Etudes Spatiales (CNES), Centre National de la Recherche Scientifique (CNRS), Institut National de Recherches Agronomiques (INRA), Institut de Recherche pour le Développement (IRD), Université Paul Sabatier, Toulouse, France, <sup>5</sup>Interactions Sol Plante Atmosphère (ISPA), Unité Mixte de Recherche 1391, Institut National de la Recherche Agronomique (INRA), Villenave d'Ornon, France, <sup>6</sup>ESA, ESRIN, Frascati, Italy, <sup>7</sup>ESA, ESTEC, Noordwijk, The Netherlands

**Abstract** The northern land biosphere is believed to be the main global sink of CO<sub>2</sub>, but the contribution of Europe is uncertain. While bottom-up estimates and inverse atmospheric transport studies based on atmospheric CO<sub>2</sub> observed in situ or from space by OCO-2 point to a moderate rate of uptake, some other inversions based on remotely sensed atmospheric CO<sub>2</sub> from GOSAT/SCIAMACHY and biomass estimates from passive microwave satellite data point to a large sink of around 1 Gt C/yr. We present results from combining both approaches in a data assimilation framework, inverting a biosphere model against in situ atmospheric CO<sub>2</sub> and passive microwave measurements. When assimilating all observations, we estimate a European carbon sink of  $0.303 \pm 0.083$  Gt C/yr for 2010–2015. The result agrees with other bottom-up studies and atmospheric inversions using in situ CO<sub>2</sub> or OCO-2 observations pointing to potential data problems when using observations from GOSAT or SCIAMACHY to estimate the European CO<sub>2</sub> sink.

## 1. Introduction

CO<sub>2</sub> is arguably the most important greenhouse gas contributing to global warming. Anthropogenic emissions of CO<sub>2</sub> currently amount to approximately 10.8 Gt C/yr of which about 3.2 Gt C/yr are taken up by land and about 2.4 Gt C/yr by oceans (Le Quéré et al., 2018). However, the exact size and location of these sinks is uncertain. Even for Europe, a region with dense networks of stations—measuring both CO<sub>2</sub> concentrations and fluxes—there is a large spread in recent estimates of the region's carbon sink (see Reuter et al., 2017, and Table 1 for an overview):  $0.27 \pm 0.16$  Gt C/yr for 2000–2005 based on a combination of bottom-up methods with atmospheric inversion against in situ CO<sub>2</sub> concentrations (Schulze et al., 2009),  $0.40 \pm 0.42$  Gt C/yr for 2001–2004 based on an ensemble of atmospheric inversions against in situ CO<sub>2</sub> concentrations (Peylin et al., 2013), and  $0.95 \pm 0.33$  Gt C/yr for 2003–2010 from an inversion against satellite (SCIAMACHY) remotely sensed total CO<sub>2</sub> column concentration (XCO<sub>2</sub>) (Reuter et al., 2014). Feng et al. (2016) found a higher uptake for Europe using GOSAT XCO<sub>2</sub> for 2010 ( $1.4 \pm 0.19$  Gt C/yr) than when using only in situ data ( $0.58 \pm 0.14$  Gt C/yr).

The higher sink estimates from inversion against XCO<sub>2</sub> observations are in agreement with a recently inferred sink based on passive microwave satellite measurements of vegetation optical depth (VOD). Liu et al. (2015) used C-band VOD (C-VOD) observations as a proxy for above-ground biomass (AGB) and related the trend in C-VOD to changes in AGB. Using this method they calculated an average European sink of  $0.88 \pm 0.1$  Gt C/yr over the years 2003–2010.

In a more recent study Kaminski et al. (2017) assimilated two XCO<sub>2</sub> products (one retrieved from GOSAT and one from SCIAMACHY) into a diagnostic biosphere model and inferred a European sink of about 0.6 Gt C in the year 2010 using either product, but for a smaller domain than the above studies. When

**Table 1**  
*European (TRANSCOM Region) CO<sub>2</sub> Sink Estimates in Gt C/yr From Various Studies (SM Refers to Soil Moisture)*

	Carbon sink	Data used	Period covered
Schulze et al. (2009)	0.27 ± 0.16	various in situ	2000–2005
Peters et al. (2010)	0.17 ± 0.44	in situ CO <sub>2</sub>	2001–2007
Peylin et al. (2013)	0.40 ± 0.42	in situ CO <sub>2</sub>	2001–2004
Reuter et al. (2014)	0.95 ± 0.33	XCO <sub>2</sub> , SCIAMACHY	2003–2010
Houweling et al. (2015)	1.03 ± 0.47	XCO <sub>2</sub> , GOSAT and in situ CO <sub>2</sub>	2009–2010
Feng et al. (2016)	1.40 ± 0.19	XCO <sub>2</sub> , GOSAT	2010
Feng et al. (2016)	0.58 ± 0.14	in situ CO <sub>2</sub>	2010
Kaminski et al. (2017)	1.08 (± 0.18) <sup>a</sup>	XCO <sub>2</sub> , GOSAT	2010
Crowell et al. (2019)	0.25 ± 0.46	XCO <sub>2</sub> , OCO-2	2015–2016
Crowell et al. (2019)	0.33 ± 0.40	in situ CO <sub>2</sub>	2015–2016
Liu et al. (2015)	0.88 ± 0.31	C-VOD	2003–2010
This study	0.30 ± 0.08	in situ CO <sub>2</sub> , SM, and L-VOD	2010–2015

<sup>a</sup>Note that Kaminski et al. (2017) provide fluxes and uncertainties for a smaller domain covering political Europe (i.e., excluding Russia); here we have extracted the flux over the Transcom region but show the uncertainty for the smaller domain with a sink of ≈0.6 Gt C/yr.

integrated over the same domain the inferred sink of about 1.1 Gt C/yr is similar to that of other studies based on GOSAT/SCIAMACHY XCO<sub>2</sub> observations. Most recently, Kountouris et al. (2018) used in situ measurements from 16 stations in a regional European atmospheric inversion system and inferred for the year 2007 a sink ranging between 0.23 ± 0.13 and 0.38 ± 0.17 Gt C/yr depending on the assumed prior uncertainty structure and also for a different domain.

Here we follow the approach by Kaminski et al. (2017) but assimilate a different combination of observational data into a process-based terrestrial ecosystem model, namely, in situ atmospheric CO<sub>2</sub>, soil moisture and L-band VOD (L-VOD), the latter two derived from the Soil Moisture Ocean Salinity (SMOS) satellite (Kerr et al., 2010). We are thus able to infer a European CO<sub>2</sub> sink consistent with both the terrestrial biosphere model and all three observational data sets. We also provide an uncertainty estimate for the sink strength consistent with the uncertainties of all observations and the model.

## 2. Methods

### 2.1. Carbon Cycle Data Assimilation

This contribution is based on the Carbon Cycle Data Assimilation System (CCDAS), a comprehensive modeling framework that combines bottom-up and top-down approaches to global carbon flux modeling. The bottom-up components are the Biosphere-Energy-Transfer-Hydrology model (BETHY, Knorr, 2000) as well as various background fluxes. The top-down component of CCDAS consists of a set of observational operators that map BETHY state variables onto observable quantities (Kaminski & Mathieu, 2017), and an assimilation algorithm that is able to adjust a control vector in order to optimize agreement with observations. This optimization algorithm relies on derivative information provided by the automatic differentiation tool TAPENADE (Hascoët & Pascual, 2013).

The data assimilation methodology of CCDAS is described in detail by Kaminski et al. (2013), and references therein. In brief, it consists of the following steps: (1) A control vector (consisting of a set of process parameters in the BETHY model and the observation operators for surface soil moisture, L-VOD, and CO<sub>2</sub>) is defined with prior values and uncertainties (see supporting information, SI). Running the model with the prior control vector yields the prior fields of surface fluxes. A linearized version of the model (Jacobian) is used to project the control vector uncertainty to flux space. (2) In an inversion step, the control vector is optimized in such a way that a cost function reflecting the deviation between observed and model simulated quantities, as well as the deviation from the prior control parameters, is minimized. The cost function takes into account uncertainties of both parameters, observations, and model results. (3) Posterior uncertainty ranges of the (optimized) control vector are estimated such that they are consistent with the uncertainties

in the prior, the model, and the observations. (4) The posterior control vector is projected onto carbon fluxes and their uncertainty ranges.

BETHY (Knorr, 2000) simulates exchange fluxes between the atmosphere and the terrestrial biosphere with an hourly time step. Computation of photosynthesis is fully embedded within the energy and water balance, which is computed separately for bare-soil and vegetated surface fractions, enabling the inclusion of feedbacks between canopy structure and the soil water balance. Input data sets are described in the SI. A number of modifications were necessary to better simulate surface soil moisture as seen by microwave radiometers. The BETHY soil water scheme was substantially revised based on the Variable Infiltration Capacity 1-layer model by (Wood et al., 1992), with a 4-cm-thick surface and a root zone layer.

In our study, BETHY simulates carbon fluxes on a global  $0.25^\circ$  by  $0.25^\circ$  grid and is run for the period 2010–2015. In addition, background carbon fluxes are prescribed for ocean-atmosphere exchange, fossil fuel burning and land use. We use temporally and spatially resolved estimates of the global air-sea CO<sub>2</sub> flux based on the Surface Ocean CO<sub>2</sub> Atlas data set (Rödenbeck et al., 2013), fossil fuel emissions from Boden et al. (2016) distributed with the spatial pattern of Brenkert (1998), and land use change emissions from (Houghton, 2003) rescaled according to recent estimates from Le Quéré et al. (2018). At each grid cell, the heterotrophic respiration is scaled to match the Net Primary Production (NPP) of a reference run. Our prior parameter set is almost identical to that used for the reference run (see SI) resulting in a prior Net Ecosystem Productivity (NEP, net CO<sub>2</sub> uptake by the terrestrial vegetation) close to 0 (quasi-neutral biosphere).

Observational operators are included for atmospheric CO<sub>2</sub> concentration at remote monitoring stations, surface soil moisture and SMOS L-VOD. The atmospheric transport model TM3 (Heimann & Körner, 2003) with approximately  $4^\circ$  by  $5^\circ$  horizontal resolution on 19 vertical levels is used to link carbon fluxes at the Earth surface to atmospheric CO<sub>2</sub> measurements. TM3 here takes monthly mean values of surface CO<sub>2</sub> fluxes to compute monthly mean CO<sub>2</sub> concentrations collected at a global station network (see SI). To maximize consistency with the measurements, the observation operator for CO<sub>2</sub> also includes a station-specific sampling schedule. Matching observations are taken from several institutions based on the Jena Carboscope (Rödenbeck, 2005). Within each month, we use the standard deviation of measured CO<sub>2</sub> concentrations with a floor value of 0.5 ppm as the combined model and observational uncertainty for CO<sub>2</sub> concentrations (see SI).

Surface volumetric soil moisture and annual L-VOD are taken from the SMOS-IC product (Fernandez-Moran et al., 2017), which provides simultaneous retrievals from measurements by a L-band (1.4 GHz) passive microwave radiometer onboard SMOS, based on the L-band Microwave Emission of the Biosphere model (Wigneron et al., 2007). Surface soil moisture retrievals are matched to simulated volumetric soil moisture of the thin surface layer of BETHY. Another observation operator describes L-VOD as the sum of an empirically derived AGB-dependent term (Rodriguez-Fernandez et al., 2018), and a term proportional to the leaf area index. AGB in turn is simulated as the product of long-term NPP and its turnover time, which is included in the CCDAS control vector that is varied in the course of the assimilation. More detail on the L-VOD observation operator is provided in the SI. Both SMOS observation operators were first tested at site scale (Kaminski et al., 2018). For assimilation, both SMOS products were mapped onto the regular  $0.5^\circ \times 0.5^\circ$  BETHY grid. The soil moisture product was aggregated to daily means from 1 July 2010 to 31 December 2015 and the L-VOD product to annual values for the years 2011 to 2015. When aggregating from the original SMOS grid (25 km × 25 km) to the BETHY grid, we assume the uncertainty of all observations within the same model grid cell to be completely correlated.

After filtering and quality control, the number of monthly atmospheric CO<sub>2</sub> data points at our 10 stations amounts to 670, the yearly L-VOD on the BETHY grid to 272,245, and the daily soil moisture data to 20,366,138 observations. The data uncertainty for both SMOS products is taken from the retrieval algorithm following the different data processing steps as explained in the SI. We assign minimum values of 0.1 for (volumetric) soil moisture and 0.04 for L-VOD. These floor values avoid very small data uncertainties, that is, a very high confidence level. We do expect data uncertainty to be correlated in space and time and between the two SMOS products. It is difficult to assess such uncertainty correlation on both sides; that is, in the observations and in the modeling chain and we are left with plausible assumptions. Technically, the effect of data uncertainty correlation is a reduced weight in the cost function and can thus be conveniently included into the formalism through an inflated data uncertainty. Inflating the uncertainty on our data set by a factor of  $\sqrt{n}$  means that we can represent it by a set of independent observations with a sample size

**Table 2**

European Flux Estimates From the Different Experiments (Reference (Prior); CO<sub>2</sub>; CO<sub>2</sub>+SMOS) in Gt C/yr and the Fit Against Different Data

Experiment	Europ. flux estimate		Data fit				Data fit 2016	
	NEP	NPP	CO <sub>2</sub> (A)	CO <sub>2</sub> (V)	SM	L-VOD	CO <sub>2</sub> (A)	CO <sub>2</sub> (V)
Prior	-0.024±1.19	4.60±0.81	40061	84323	0.127	0.130	20718	38788
CO <sub>2</sub>	0.18±0.12	4.82±0.16	631	2059	0.117	0.145	101	252
CO <sub>2</sub> +SMOS	0.30±0.08	4.82±0.12	722	2264	0.113	0.103	134	257

Note. For CO<sub>2</sub> the fit is expressed as the respective data term in the cost function, whereas for soil moisture (SM) and L-VOD as RMSE. The last two columns (Data fit 2016) show the fit against CO<sub>2</sub> observations for an additional validation year 2016 outside the assimilation period (2010–2015). Note that CO<sub>2</sub> (A) refers to assimilated atmospheric CO<sub>2</sub> observations and CO<sub>2</sub> (V) to those withheld from the assimilation, hence, data used for evaluation and not in the assimilation.

(that is, an “effective sample size”, see Cressie, 1960) that is a factor of  $n$  smaller. For the uncertainty correlation between the two variables and in space, we increase the data uncertainty by a factor of  $\sqrt{100}$  (fully independent samples at 5° × 5°). Furthermore, for the daily soil moisture product we take uncertainty correlation in time into account through an extra multiplier of  $\sqrt{75}$ . This procedure reduces the weight of the L-VOD data in the cost function to that of 2,722 (1/100th) fully independent data points and the weight of the soil moisture data to that of 2,715 (1/7500th) fully independent data points. More details on the uncertainty specification is given in the SI.

To assess the results of our assimilation experiments we compare the results against atmospheric CO<sub>2</sub> observations from additional monitoring stations not used during assimilation.

## 2.2. Experiments

We performed the following experiments at global scale (Table 2):

- CO<sub>2</sub>: assimilation of in situ observations of atmospheric CO<sub>2</sub>
- CO<sub>2</sub>+SMOS: simultaneous assimilation of in situ observations of atmospheric CO<sub>2</sub> with the SMOS soil moisture and L-VOD products

By performing forward simulations with BETHY using the optimal parameter values from the assimilation experiments, we obtain gross and net carbon fluxes at a 0.25° spatial and monthly temporal resolution that are consistent with the observations and their uncertainties (see SMOS+Veg Study Team, 2019, for posterior NEP with uncertainty estimates from the CO<sub>2</sub>+SMOS experiment). We also perform a simulation with the prior control vector. For all three runs we provide carbon fluxes and uncertainties integrated over the European TRANSCOM region (Gurney et al., 2002).

## 3. Results and Discussion

At the global scale, the mean annual NEP is very similar between the two assimilation experiments, namely, 3.98 Gt C/yr for the CO<sub>2</sub> and 3.96 Gt C/yr for the CO<sub>2</sub>+SMOS experiment during 2010 to 2015. This is because the global terrestrial sink over our simulation period is determined by the global atmospheric CO<sub>2</sub> growth rate since all the other exchange (background) fluxes are prescribed as mentioned in section 2.1. The same does not apply when considering a region like Europe. For the CO<sub>2</sub> experiment, we find a small sink that is not significantly different from 0, but a moderate sink of 0.30 ± 0.08 Gt C/yr for the CO<sub>2</sub>+SMOS experiment. At the same time, the uncertainty estimate for the European sink is greatly reduced for the CO<sub>2</sub> experiment compared to the prior case, and even further, by an additional 26%, for the CO<sub>2</sub>+SMOS experiment (Table 2). We also infer a European NPP slightly higher (4.8 Gt C/yr) for CO<sub>2</sub> and CO<sub>2</sub>+SMOS compared to the prior simulation (4.6 Gt C/yr), and with much reduced uncertainty. The main contribution ( $\approx 2/3$ ) to the sink in the CO<sub>2</sub>+SMOS experiment results from the increase in NPP of  $\approx 0.2$  Gt C/yr compared to the prior case. The remaining contribution to the sink ( $\approx 1/3$ ) for CO<sub>2</sub>+SMOS is the result of a lower respiration. The slightly smaller sink of the CO<sub>2</sub> experiment is caused by a slightly higher respiration compared to the CO<sub>2</sub>+SMOS experiment, because NPP is equal for both experiments.

Both experiments (CO<sub>2</sub> and CO<sub>2</sub>+SMOS) have resulted in a considerable reduction of the cost function as evidenced by an improved fit against the assimilated data (see Table 2). Compared to the quasi-neutral

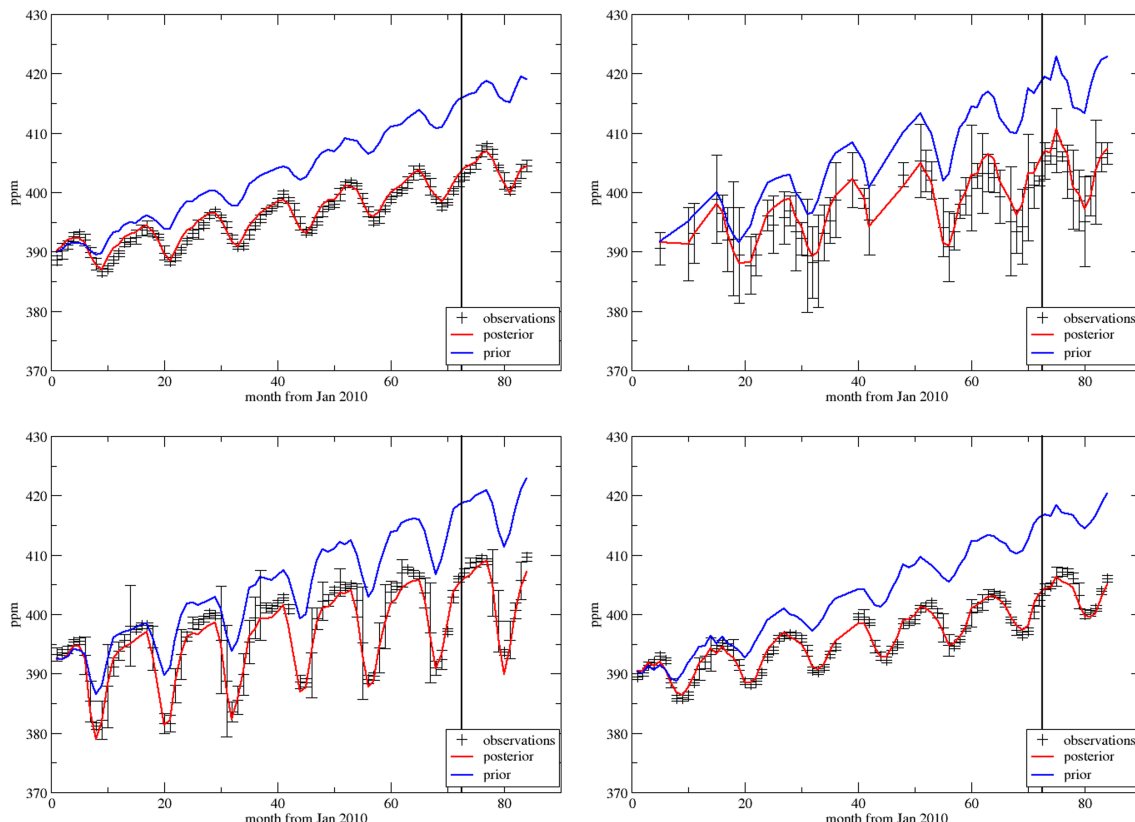


**Figure 1.** Atmospheric CO<sub>2</sub> concentrations at two stations used in the assimilation (left column: Mauna Loa, Hawaii (top) and Alert, Canada (bottom)) and at two stations used for validation (excluded from the assimilation; right column: Monte Cimone, Italy (top) and Assekrem, Algeria (bottom)). Note that the last 12 months show the results for the validation year 2016 outside the assimilation period (2010–2015). The posterior concentrations shown in the graphs are from the CO<sub>2</sub>+SMOS experiment.

prior both experiments achieve a much better fit of the trend in the atmospheric CO<sub>2</sub> observations. But the agreement of shape and timing of interannual and intra-annual CO<sub>2</sub> fluctuations has also improved, and the agreement with CO<sub>2</sub> stations excluded from assimilation (validation stations) is improved to the same degree. Figure 1 shows the fit against the CO<sub>2</sub> observations for the CO<sub>2</sub>+SMOS experiment for two stations used in the assimilation (left) and for two validation stations that are located close to Europe (right) as well as for an additional validation year (2016) beyond the assimilation period; for all cases there is a remarkably good agreement between the simulated concentrations and the observations in terms of long-term trend but also seasonality (more validation stations are shown in the SI).

As expected, surface soil moisture and L-VOD agree notably better for the CO<sub>2</sub>+SMOS compared to the prior simulation. For the CO<sub>2</sub> experiment, soil moisture agrees better compared to the prior case, even though it was not assimilated. The improvement in L-VOD is more pronounced than that for soil moisture, with an almost 30% reduction in the root-mean-square error for the CO<sub>2</sub>+SMOS experiment as compared to the CO<sub>2</sub> experiment, which achieves a slightly worse fit than in the prior case (see SI for difference maps of the mean simulated soil moisture and L-VOD with the SMOS IC products used in the assimilation).

The inferred European sink for the CO<sub>2</sub>+SMOS experiment is close to the combined bottom-up/top-down estimate of Schulze et al. (2009), but substantially below those of using XCO<sub>2</sub> from GOSAT or SCIAMACHY. It is also below the estimate from the study based on C-band VOD by Liu et al. (2015), using microwaves at a shorter wavelength (Table 1). Our estimate is also lower than the sink inferred by Kaminski et al. (2017), who used a CCDAS with a diagnostic terrestrial biosphere model and assimilated XCO<sub>2</sub> observations from both GOSAT and SCIAMACHY.

Figure 2 shows maps of the mean annual NEP (left) and NPP (right) from the CO<sub>2</sub>+SMOS experiment over Europe. Areas of a strong carbon sink tend to be colocated with areas of high NPP, mainly the UK and western to central Europe (parts of France, Benelux, Germany, Poland, Ukraine, and parts of Russia).

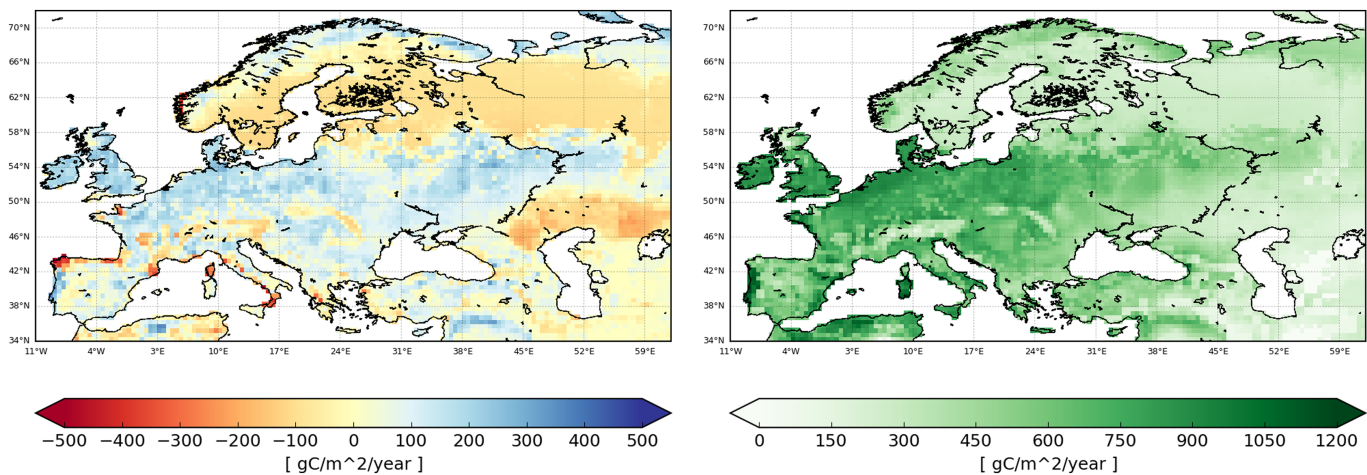


**Figure 2.** Annual CO<sub>2</sub> fluxes averaged over the period 2010 to 2015 from the CO<sub>2</sub>+SMOS assimilation experiment for NEP (left, positive is a sink) and NPP (right).

Most prominent is a carbon source band extending from Scandinavia eastward into Russia in contrast to Kaminski et al. (2017) who simulated, with a different model and assimilating GOSAT XCO<sub>2</sub> observations, this area as a carbon sink. While in the CO<sub>2</sub> experiment this region results in a small sink (not shown here), it becomes a source when assimilating also the SMOS observations. The reason is a downward adjustment of the productivity of boreal trees (PFT 5) to bring simulated L-VOD more in line with SMOS observations (see also Figure S7 in the SI). Other studies, such as Reuter et al. (2014) and Houweling et al. (2015), that base their results on inversions using GOSAT or SCIAMACHY XCO<sub>2</sub> observations claim that Northeastern Europe (50–70°N, 30–60°E) contributes most to their larger estimate of the European carbon sink.

According to Feng et al. (2016) the higher sink estimates from the inversion of XCO<sub>2</sub> could either be explained by biases in the XCO<sub>2</sub> observations used in these studies—provided by GOSAT and SCIAMACHY—or an overestimation of the net CO<sub>2</sub> flux transported into the European domain from outside the region and thus resulting in an overestimation of the sink in the domain. A recent study based on an ensemble of atmospheric inversion systems using OCO-2 land nadir and land glint XCO<sub>2</sub> as well as in situ observations resulted in only moderate sink estimates for 2015–2016 (Crowell et al., 2019), with an ensemble mean of 0.25 Gt C/yr (range 0.46 Gt C/yr) for land nadir, 0.36 Gt C/yr (range 0.40 Gt C/yr) for land glint, and 0.33 Gt C/yr (range 0.4 Gt C/yr) for in situ observations provided by the GLOBALVIEW+ project (Cooperative Global Atmospheric Data Integration Project, 2017). These estimates are in good agreement with our estimate and also substantially lower than the ones based on SCIAMACHY and GOSAT XCO<sub>2</sub> observations.

Apart from those, only Liu et al. (2015) report a larger European sink strength, based on trends in C-VOD data from remotely sensed passive microwave observations as a proxy for changes in AGB. However, the relationship between AGB and C-VOD saturates and C-VOD becomes only weakly sensitive to AGB changes in the range ≈50 to ≈250 Mg/ha, which is a typical range for European forest ecosystems (Brandt et al., 2018; Rodríguez-Fernández et al., 2018).

#### 4. Conclusions

This study offers a new perspective on the land carbon cycle, because it is the first time to achieve the simultaneous assimilation of three observational data products into a model of the terrestrial biosphere. By assimilating both atmospheric CO<sub>2</sub> and passive microwave observations, it combines the two main data sources whose analysis has so far shaped the debate on the strength of the European carbon sink, but it also adds process-based knowledge typical of bottom-up (model based) studies. Posterior fluxes reproduce observed CO<sub>2</sub> variability at several stations close to Europe that were not included in the assimilation. Using all three data sets for assimilation, we estimate the European sink to be significantly larger than 0, but only of moderate strength and well below 1 Gt C/yr as reported by some studies. The study also documents the potential of passive microwave data in the L-band to further constrain regional carbon flux estimates, as the posterior uncertainty of the combined CO<sub>2</sub> and microwave data assimilation was considerably smaller than for CO<sub>2</sub> only.

We evaluate our results by assessing the fit against the assimilated data sets as well as independent data. The evaluation against atmospheric CO<sub>2</sub> measurements from stations withheld from the assimilation as well as an additional simulation year outside the assimilation period shows an excellent agreement of the simulated concentration with the observations, and in particular also at stations close to Europe indicating that our simulated fluxes are consistent with the atmospheric observations.

What is emerging is a close agreement among our study, with a largely different approach, and both bottom-up and inversion studies using either in situ CO<sub>2</sub> or OCO-2 XCO<sub>2</sub> data. This is contrasted with an equally close agreement among studies that use GOSAT or SCIAMACHY XCO<sub>2</sub> either in atmospheric inversions, or in a CCDAS, who all report a much larger sink. This general picture is a strong indicator that there might be an inherent bias contained in the available XCO<sub>2</sub> data sets from those two satellites, as suspected by Feng et al. (2016). The only independent support for a larger European sink strength comes from C-band microwave data used to estimate changes in AGB. It therefore remains to be seen whether future studies inferring the European strength from biomass changes based on longer-wavelength L-band data will also estimate a moderate sink strength, similar to the present study, also using L-band microwave data. This is relevant, because L-band microwaves penetrate considerably deeper into forest canopies than C-band, and therefore are less prone to signal saturation (Brandt et al., 2018; Rodríguez-Fernández et al., 2018).

As a way to further address if indeed GOSAT and SCIAMACHY XCO<sub>2</sub> are responsible for reports of a large European sink we propose to assimilate CO<sub>2</sub> data obtained from either in situ measurements, GOSAT and SCIAMACHY XCO<sub>2</sub>, or OCO-2 XCO<sub>2</sub>, similar to (Crowell et al., 2019), but in a data assimilation framework and combined with the assimilation of L-band observations. If in such a configuration the same dichotomy appears between in situ and OCO-2, and GOSAT and SCIAMACHY, it will appear most likely that some bias problem is to be addressed for the latter data sets. We note here that such a data assimilation system with a process-based model at its core constitutes an ideal platform for consistently integrating various data sets, that is, the approach here can be extended to integrate data from a virtual carbon satellite constellation encompassing the atmospheric (XCO<sub>2</sub>), physical land surface (soil moisture and land surface temperature), and biogeochemical land surface (biomass, fraction of absorbed photosynthetically active radiation, FAPAR) components.

## References

**Acknowledgments**  
This study was funded by the European Space Agency's Support to Science Element under Contract 4000117645/16/NL/SW. M. S., W. K., and M. W. acknowledge additional support from the Swedish National Space Agency (Dnr 102/14) and the EU VERIFY project (Grant Agreement (GA): 776810). The resulting data from this study is available at the ICOS Carbon Portal (under <https://doi.org/10.18160/yd1g-4trq>).

- Boden, T., Marland, G., & Andres, R. (2016). *Global, regional, and national fossil-fuel CO<sub>2</sub> emissions*. Oak Ridge, Tenn, U.S.A: Carbon Dioxide Information Analysis Center, Oak Ridge National Laboratory, U.S. Department of Energy. [https://doi.org/10.3334/CDIAC/00001\\_V2016](https://doi.org/10.3334/CDIAC/00001_V2016)
- Brandt, M., Wigneron, J. P., Chave, J., Tagesson, T., Penuelas, J., Ciais, P., et al. (2018). Satellite passive microwaves reveal recent climate-induced carbon losses in African drylands. *Nature Ecology & Evolution*, 2(5), 827–835. <https://doi.org/10.1038/s41559-018-0530-6>
- Brenkert, A. L. (1998). Carbon dioxide emission estimates from fossil-fuel burning, hydraulic cement production, and gas flaring for 1995 on a one degree grid cell basis. Retrieved from <http://cdiac.esd.ornl.gov/ndps/ndp058a.html>
- Cooperative Global Atmospheric Data Integration Project (2017). Multi-laboratory compilation of atmospheric carbon dioxide data for the period 1957–2016. NOAA Earth System Research Laboratory, Global Monitoring Division <https://doi.org/10.15138/G3704H>
- Cressie, A. C. (1960). *Statistics for spatial data*. New York: Wiley.
- Crowell, S., Baker, D., Schuh, A., Basu, S., Jacobson, A. R., Chevallier, F., et al. (2019). The 2015–2016 carbon cycle as seen from OCO-2 and the global in situ network. *Atmospheric Chemistry and Physics Discussions*, 2019, 1–79. <https://doi.org/10.5194/acp-2019-87>
- Feng, L., Palmer, P. I., Parker, R. J., Deutscher, N. M., Feist, D. G., Kivi, R., et al. (2016). Estimates of European uptake of CO<sub>2</sub> inferred from GOSAT XCO<sub>2</sub> retrievals: Sensitivity to measurement bias inside and outside Europe. *Atmospheric Chemistry and Physics*, 16(3), 1289–1302. <https://doi.org/10.5194/acp-16-1289-2016>
- Fernandez-Moran, R., Al-Yaari, A., Mialon, A., Mahmoodi, A., Al Bitar, A., De Lannoy, G., et al. (2017). SMOS-IC: An alternative SMOS soil moisture and vegetation optical depth product. *Remote Sensing*, 9(5). <https://doi.org/10.3390/rs9050457>
- Gurney, K. R., Law, R. M., Denning, A. S., Rayner, P. J., Baker, D., Bousquet, P., et al. (2002). Towards robust regional estimates of CO<sub>2</sub> sources and sinks using atmospheric transport models. *Nature*, 415, 626–630.
- Hascoët, L., & Pascual, V. (2013). The tapenade automatic differentiation tool: Principles, model, and specification. *ACM Transactions On Mathematical Software*, 39(3), 20:1–20:43. <https://doi.org/10.1145/2450153.2450158>
- Heimann, M., & Körner, S. (2003). The global atmospheric tracer model TM3 (5). Jena, Germany: Max-Planck-Institut für Biogeochemie.
- Houghton, R. A. (2003). Revised estimates of the annual net flux of carbon to the atmosphere from changes in land use and land management 1850–2000. *Tellus B*, 55(2), 378–390.
- Houweling, S., Baker, D., Basu, S., Boesch, H., Butz, A., Chevallier, F., et al. (2015). An intercomparison of inverse models for estimating sources and sinks of CO<sub>2</sub> using GOSAT measurements. *Journal of Geophysical Research: Atmospheres*, 120, 5253–5266. <https://doi.org/10.1002/2014JD022962>
- Kaminski, T., Knorr, W., Schürmann, G., Scholze, M., Rayner, P. J., Zaehle, S., et al. (2013). The BETHY/JSBACH carbon cycle data assimilation system: Experiences and challenges. *Journal of Geophysical Research: Biogeosciences*, 118, 1414–1426. <https://doi.org/10.1002/jgrg.20118>
- Kaminski, T., & Mathieu, P. P. (2017). Reviews and syntheses: Flying the satellite into your model: On the role of observation operators in constraining models of the Earth system and the carbon cycle. *Biogeosciences*, 14(9), 2343–2357. <https://doi.org/10.5194/bg-14-2343-2017>

- Kaminski, T., Scholze, M., Knorr, W., Vossbeck, M., Wu, M., Ferrazzoli, P., et al. (2018). Constraining terrestrial carbon fluxes through assimilation of SMOS products, IGARSS 2018 - 2018 IEEE International Geoscience and Remote Sensing Symposium, pp. 1455–1458. <https://doi.org/10.1109/IGARSS.2018.8518724>
- Kaminski, T., Scholze, M., Vossbeck, M., Knorr, W., Buchwitz, M., & Reuter, M. (2017). Constraining a terrestrial biosphere model with remotely sensed atmospheric carbon dioxide. *Remote Sensing of Environment*, 203, 109–124. <https://doi.org/10.1016/j.rse.2017.08.017>
- Kerr, Y., Waldteufel, P., Wigneron, J. P., Delwart, S., Cabot, F., Boutin, J., et al. (2010). The SMOS mission: New tool for monitoring key elements of the global water cycle. *Proceedings of the IEEE*, 98(5), 666–687. <https://doi.org/10.1109/JPROC.2010.2043032>
- Knorr, W. (2000). Annual And interannual CO<sub>2</sub> exchanges of the terrestrial biosphere: Process-based simulations and uncertainties. *Global Ecology and Biogeography*, 9(3), 225–252.
- Kountouris, P., Gerbig, C., Rödenbeck, C., Karstens, U., Koch, T. F., & Heimann, M. (2018). Atmospheric CO<sub>2</sub> inversions on the mesoscale using data-driven prior uncertainties: Quantification of the European terrestrial CO<sub>2</sub> fluxes. *Atmospheric Chemistry and Physics*, 18(4), 3047–3064. <https://doi.org/10.5194/acp-18-3047-2018>
- Le Quéré, C., Andrew, R. M., Friedlingstein, P., Sitch, S., Pongratz, J., Manning, A. C., et al. (2018). Global carbon budget 2017. *Earth System Science Data*, 10(1), 405–448. <https://doi.org/10.5194/essd-10-405-2018>
- Liu, Y. Y., van Dijk, A. I. J. M., de Jeu, R. A. M., Canadell, J. G., McCabe, M. F., Evans, J. P., & Wang, G. (2015). Recent reversal in loss of global terrestrial biomass. *Nature Climate Change*, 5, 470–474. <https://doi.org/10.1038/nclimate2581>
- Peters, W., Krol, M. C., van der Werf, G. R., Houweling, S., Jones, C. D., Hughes, J., et al. (2010). Seven years of recent European net terrestrial carbon dioxide exchange constrained by atmospheric observations. *Global Change Biology*, 16(4), 1317–1337. <https://doi.org/10.1111/j.1365-2486.2009.02078.x>
- Peylin, P., Law, R. M., Gurney, K. R., Chevallier, F., Jacobson, A. R., Maki, T., et al. (2013). Global atmospheric carbon budget: Results from an ensemble of atmospheric CO<sub>2</sub> inversions. *Biogeosciences*, 10(10), 6699–6720. <https://doi.org/10.5194/bg-10-6699-2013>
- Reuter, M., Buchwitz, M., Hilker, M., Heymann, J., Bovensmann, H., Burrows, J. P., et al. (2017). How much CO<sub>2</sub> is taken up by the European terrestrial biosphere? *Bulletin of the American Meteorological Society*, 98(4), 665–671. <https://doi.org/10.1175/BAMS-D-15-00310.1>
- Reuter, M., Buchwitz, M., Hilker, M., Heymann, J., Schneising, O., Pillai, D., et al. (2014). Satellite-inferred European carbon sink larger than expected. *Atmospheric Chemistry and Physics*, 14(24), 13,739–13,753. <https://doi.org/10.5194/acp-14-13739-2014>
- Rödenbeck, C. (2005). Estimating CO<sub>2</sub> sources and sinks from atmospheric mixing ratio measurements using a global inversion of atmospheric transport (06). Jena, Germany: Max-Planck-Institut für Biogeochemie.
- Rödenbeck, C., Keeling, R. F., Bakker, D. C. E., Metzl, N., Olsen, A., Sabine, C., & Heimann, M. (2013). Global surface-ocean pCO<sub>2</sub> and sea-air CO<sub>2</sub> flux variability from an observation-driven ocean mixed-layer scheme. *Ocean Science*, 9(2), 193–216. <https://doi.org/10.5194/os-9-193-2013>
- Rodríguez-Fernández, N. J., Mialon, A., Mermoz, S., Bouvet, A., Richaume, P., Al Bitar, A., et al. (2018). An evaluation of SMOS L-band vegetation optical depth (L-VOD) data sets: High sensitivity of L-VOD to above-ground biomass in Africa. *Biogeosciences*, 15(14), 4627–4645. <https://doi.org/10.5194/bg-15-4627-2018>
- Rodríguez-Fernandez, N., Mialon, A., Mermoz, S., Bouvet, A., Richaume, P., Bitar, A. A., et al. (2018). SMOS L-band vegetation optical depth is highly sensitive to aboveground biomass. In *2018 IEEE International Geoscience and Remote Sensing Symposium (IGARSS)*.
- SMOS+Veg Study Team (2019). BETHY global Net Ecosystem Production (NEP) maps at 0.25 degree resolution for the period 2010–2015. <https://doi.org/10.18160/ysdg-4trq>
- Schulze, E. D., Luysaert, S., Ciais, P., Freibauer, A., Janssens, I. A., Soussana, J. F., et al. the CarboEurope Team (2009). Importance of methane and nitrous oxide for Europe's terrestrial greenhouse-gas balance. *Nature Geoscience*, 2, 842–850. <https://doi.org/10.1038/ngeo686>
- Wigneron, J. P., Kerr, Y., Waldteufel, P., Saleh, K., Escorihuela, M. J., Richaume, P., et al. (2007). L-band Microwave Emission of the Biosphere (L-MEB) model: Description and calibration against experimental data sets over crop fields. *Remote Sensing of Environment*, 107(4), 639–655. <https://doi.org/10.1016/j.rse.2006.10.014>
- Wood, E., Lettenmaier, D., & Zartarian, V. (1992). A land-surface hydrology parameterization with subgrid variability for general circulation models. *Journal of Geophysical Research*, 97, 2717–2728.